A novel model for the simulation of chaos in low-flow-rate CSTR experiments with the Belousov-Zhabotinsky reaction: A chemical mechanism for two frequency oscillations

ARTICLE *in* THE JOURNAL OF PHYSICAL CHEMISTRY · APRIL 1991

Impact Factor: 2.78 · DOI: 10.1021/j100161a038

3 AUTHORS, INCLUDING:

Susan B Rempe
Sandia National Laboratories
102 PUBLICATIONS **1,705** CITATIONS

A Novel Model for the Simulation of Chaos in Low-Flow-Rate CSTR Experiments with the Belousov–Zhabotinsky Reaction: A Chemical Mechanism for Two Frequency Oscillations

László Györgyi,*,† Susan L. Rempe, and Richard J. Field*

Department of Chemistry, University of Montana, Missoula, Montana 59812, and Institute of Inorganic and Analytical Chemistry, Eötvös Lóránd University, Budapest, Hungary *(Received: June 27, 1990; In Final Form: November 8, 1990)*

Continuous-flow, stirred tank reactor (CSTR) experiments with the oscillatory Belousov–Zhabotinsky (BZ) reaction provide the most important examples of chemical chaos. Experiments performed at low flow rates at the University of Texas in Austin are particularly important because of the large amount of data accumulated and the apparent low dimensionality of the attractor. Although the mechanism of the BZ reaction is largely elucidated, it has not been previously possible to simulate this aperiodicity by using realistic models of the homogeneous dynamics of the BZ system. We present here such a model based on the interaction of two frequency sources within the homogeneous flow system. One frequency is that of the Oregonator core of the model. The other originates in the dynamics of the major bromide ion precursor, bromomalonic acid (BrMA), which is a product of the overall reaction as well as a bifurcation parameter of the Oregonator core. Its concentration remains high but undergoes small-amplitude oscillations. There is a critical value of [BrMA] above which the reduced steady state of the Oregonator core becomes stable, causing [BrMA] to decrease because it is not produced in significant amounts in this state but is still washed out in a first-order manner by the flow. This negative feedback of [BrMA] on itself establishes a second frequency source within the homogeneous BZ dynamics. The interaction of the two frequencies creates the complex dynamics observed. The model, consisting of 11 dynamic variables and 19 reactions, simulates very well for the experimental conditions the observed series of major periodic states, the bifurcations of these states to chaos, and the presence of periodic–chaotic windows. Both the simulated waveforms and their next-maximum maps agree well with the measured ones. Several regions of hysteresis and very long transients also are observed in the simulations.

Oscillating chemical reactions are of great interest as relatively simple, real examples of far-from-equilibrium[1a] systems exhibiting a number of phenomena governed by nonlinear dynamic laws.[1b] The Ce(IV)/Ce(III)-catalyzed oxidation and bromination of malonic acid (MA) by BrO_3^- in $\approx$1 M H_2SO_4, the classic Belousov–Zhabotinsky (BZ) reaction,[2] is the most thoroughly studied oscillating chemical reaction. Sustained oscillation of [Ce(IV)]/[Ce(III)] and [Br^-] may be observed in a closed, well-stirred reactor. More complicated behaviors including very complex periodicity, multistability, hysteresis, and even chaos may occur[3] in a continuous-flow, stirred tank reactor (CSTR). The flow both maintains the system far from equilibrium and couples with the chemical dynamics to increase the variety and complexity of behaviors observed. We are concerned here with the source of chaos in the chemistry of BZ-CSTR experiments.

Aperiodic oscillation was first reported in BZ-CSTR experiments by Schmitz et al.[4] in 1977. Several robust and well-characterized aperiodic regimes have been discovered[5-11] since then at both low and high CSTR flow rates. A set of aperiodic experiments performed by various researchers[11-13] at the University of Texas in Austin (referred to as the "Texas chaos") appear to be the most reliable and best documented. The aperiodicity is identified[11] as deterministic chaos by reconstruction of the attractor, maps[14] derived from the attractor, and the characteristics of the transitions from periodicity to aperiodicity as the flow rate is varied. The basic outline of the Texas experiments has been reproduced by Münster and Schneider.[15]

The dynamic source of BZ-CSTR chaos is of considerable interest but has been elusive.[16,17] It is very difficult to infer the chemical source of the chaos from experimental data because only one or two of the many oscillatory intermediate concentrations are observed experimentally. Thus, most attempts to understand BZ-CSTR chaos have involved simulations based on simplified BZ mechanisms such as the Hopf-hysteresis[18] model, the reversible Oregonator,[19] or the Showalter, Noyes, Bar-Eli[20,21] model. Outdated rate constant values were used in all these cases. Although chaotic waveforms were found in these studies, they appeared only in very small flow rate ranges[18] or the calculated concentrations of Br_2, Br^-, or HOBr were unrealistically high or low.[18,19,21] Recent important simulations by Lindberg et al.[22] did

* Authors to whom correspondence should be addressed.
† Eötvös Lóránd University.

(1) (a) Nicolis, G.; Prigogine, I. *Self-Organization in Nonequilibrium Systems*; Wiley: New York, 1977. (b) Field, R. J.; Schneider, F. W. *J. Chem. Educ.* **1989**, *66*, 195.
(2) Belousov, B. P. In *Sbornik Referatov po Radiatsionnoi Meditsine*; Medgiz: Moscow, 1958; p 145 (in Russian). Zhabotinsky, A. M. *Biofizika* **1964**, *9*, 306 (in Russian).
(3) De Kepper, P.; Boissonade, J. In *Oscillations and Traveling Waves in Chemical Systems*; Field, R. J., Burger, M., Eds.; Wiley-Interscience: New York, 1985; Chapters 7.4 and 7.5.1 and references therein.
(4) Schmitz, R. A.; Graziani, K. R.; Hudson, J. L. *J. Chem. Phys.* **1977**, *67*, 3040.
(5) Hudson, J. L.; Hart, M.; Marinko, D. *J. Chem. Phys.* **1979**, *71*, 1601.
(6) Hudson, J. L.; Mankin, J. C. *J. Chem. Phys.* **1981**, *74*, 6171.
(7) Roux, J. C.; Turner, J. S.; McCormick, W. D.; Swinney, H. L. In *Nonlinear Problems: Present and Future*; Bishop, A. R., Campbell, D. K., Nicolaenko, B., Eds.; North-Holland: Amsterdam, 1982; p 409.
(8) Roux, J. C.; Rossi, A.; Bachelart, S.; Vidal, C. *Phys. Lett.* **1980**, *77A*, 391.
(9) Pomeau, Y.; Roux, J. C.; Rossi, A.; Bachelart, S.; Vidal, C. *J. Phys. Lett.* **1981**, *42*, L271.
(10) Argoul, F.; Arneodo, A.; Richetti, P.; Roux, J. C. *J. Chem. Phys.* **1987**, *86*, 3325.
(11) Roux, J. C.; Simoyi, R. H.; Swinney, H. L. *Physica D* **1983**, *8D*, 257.
(12) Coffman, K. G.; McCormick, W. D.; Noszticzius, Z.; Simoyi, R. H.; Swinney, H. L. *J. Chem. Phys.* **1987**, *86*, 119.
(13) Noszticzius, Z.; McCormick, W. D.; Swinney, H. L. *J. Phys. Chem.* **1987**, *91*, 5129. Noszticzius, Z.; McCormick, W. D.; Swinney, H. L. *J. Phys. Chem.* **1989**, *93*, 2796.
(14) We use the term "map" loosely here and elsewhere since we do not require these curves to be single valued.
(15) Münster, A.; Schneider, F. W. *J. Phys. Chem.*, submitted for publication. Schneider, F. W. Personal communication.
(16) Györgyi, L.; Field, R. J. *J. Phys. Chem.* **1988**, *92*, 7081.
(17) Györgyi, L.; Field, R. J. *J. Phys. Chem.* **1989**, *93*, 2865.
(18) Richetti, P.; Roux, J. C.; Argoul, F.; Arneodo, A. *J. Chem. Phys.* **1987**, *86*, 3339.
(19) Turner, J. S.; Roux, J. C.; McCormick, W. D.; Swinney, H. L. *Phys. Lett. A* **1981**, *85A*, 9. Ringland, J.; Turner, J. S. *Ibid.* **1984**, *105A*, 93.
(20) Showalter, K.; Noyes, R. M.; Bar-Eli, K. *J. Chem. Phys.* **1978**, *69*, 2514.
(21) Barkley, D.; Ringland, J.; Turner, J. S. *J. Chem. Phys.* **1987**, *87*, 3812.

0022-3654/91/2095-3159$02.50/0

reproduce the basic features of the experimental chaos but also suffered from unreasonable values of [HOBr] and used outdated rate constant values with feedstream concentrations different from the experimental.

The BZ chemistry can be broken down into two major parts.[23,24] The first involves the inorganic chemistry of the oxidation of Ce(III) by BrO_3^- to yield Ce(IV), HOBr, and Br_2. The second involves the mainly organic chemistry of the reactions of malonic acid (MA) and its derivatives, especially bromomalonic acid (BrMA), with Br_2, HOBr, and Ce(IV) to yield Ce(III) and Br^-, the latter of which serves as the major control intermediate[23,25] in the oscillations. The models used in previous attempts to reproduce BZ-CSTR chaos represented the BZ inorganic chemistry reasonably well but did not treat the organic chemistry in any detail. The unrealistically high concentrations of HOBr mentioned above resulted from ignoring the Br_2 hydrolysis equilibrium and the reactions of HOBr and Br_2 with MA. The very complex reaction of Ce(IV) with MA, BrMA, and their derivatives to yield Ce(III) and Br^- was represented by a single stoichiometry such as the following:

$$\text{Ce(IV)} \rightarrow \text{Ce(III)} + f\text{Br}^- \qquad \text{(I)}$$

The concentrations of major organic components are taken into the rate constant (usually referred to as k_5) of this reaction and into f, which is a stoichiometric factor controlling how many Br^- appear for each Ce(IV) that disappears. We refer to the inorganic subset of the mechanism together with reaction I as the Oregonator core of the BZ reaction. The values of k_5 and f are major bifurcation parameters[26] of the Oregonator core and are used in theoretical investigation of these models.

We have attempted[16,17] to devise chemically reasonable but reduced models of the BZ reaction with a potential source of chaos built into it. Some hint of the dynamical source of the experimental chaos was required to do this.

A common source of chaos in dynamical systems is periodic forcing[27a] or coupling[27b] of two relatively independent oscillators. Furthermore, much of the experimental behavior of BZ-CSTR chaos is interpretable in terms of two-frequency motion on a wrinkled torus.[10,21] Chaos is easily obtained and simulated when two independent BZ oscillators are electrically coupled.[28]

There are two ways in which two independent frequencies can emerge in a CSTR model of the BZ reaction. The first involves a product of the Oregonator core oscillations which affects some bifurcation parameters of the Oregonator core. Complexity including chaos may be expected if the concentration of this product oscillates in such a way that one or more bifurcation parameters move back and forth across a bifurcation border and if these oscillations have a fundamental frequency different from that of the Oregonator core. Thus, we tried[16] to simulate BZ-CSTR chaos by parametrizing f through [HOBr] (a precursor of BrMA) under conditions such that the value of f oscillated around a high-f bifurcation border. These conditions correspond to high [BrMA] and are thus compatible with the low-flow-rate nature of the Texas experiments where large concentrations of products will accumulate. We refer to this as *internal coupling* of two frequency sources within the homogeneous chemical dynamics. While previous simulations based on this approach produced complex waveforms, chaos was never observed.[16] The two frequencies always entrained, presumably because their sources were not sufficiently independent of each other.

The second method of obtaining a coupled-frequencies model of BZ-CSTR chaos is based on the observation that the appearance and characteristics of experimental chaos depend on stirring rate[10] and reactor configuration. Indeed, stirring effects are now recognized[29] as important factors in CSTR experiments involving oscillating chemical reactions. Their source is presumed to be concentration heterogeneities resulting from the finite time required for the feedstreams to mix into the CSTR contents. This process has been investigated[29] by using macromixing models of the coupling of segregated volumes with each other and with the well-mixed bulk. It is possible to reproduce the gross features of the Texas chaos by such a model[17,30] in which the primary coupling is between the well-mixed bulk and very small areas near or in the inlet ports. The model yielded waveforms and one-dimensional maps very similar to experiment, as well as all of the observed routes from periodicity to chaos. We refer to this approach as *external coupling* of two independent frequency sources.

The problems with using internal coupling to reproduce the Texas chaos combined with the observed stirring effects suggested that external coupling was the source of the aperiodicity. The chaotic parametrization of the SNB model[20] by Lindberg et al.,[22] however, prompted some rethinking. In this internal coupling model the concentration of a product, HOBr, serves[31] as a second frequency source as described above and is coupled with the Oregonator core of the SNB model through the reversibility of reaction II, which is quite strong with the set of rate constants

$$\text{Br}^- + \text{BrO}_3^- + 2\text{H}^+ \rightleftarrows \text{HOBr} + \text{HBrO}_2 \qquad \text{(II)}$$

used by these authors. In the real system, however, HOBr is quickly removed by reaction with Br^- and MA, and reaction II is not strongly reversible with the correct[32] rate constants. Nevertheless, the Lindberg et al. simulations did suggest that the internal coupling approach should be reinvestigated by using a more elaborate version of the organic chemistry.

The Model

The mechanism devised to implement internal coupling is shown in Table I and consists of 19 reactions involving 11 dynamic concentration variables. Its organic chemistry is a subset of a large model recently proposed[24] by us and only considers reactions involving malonic acid, bromomalonic acid, and malonyl radical (MA•). This is the top of the oxidative cascade of MA to CO_2. The control effect of MA•[33,34] is neglected as the Texas experiments were run without oxygen removal and did not show the effects expected with changing $[O_2]$ if control by a radical species were important. The high [BrMA] and low $[H_2SO_4]$ used in the Texas experiments also suggest[24] that MA• control should not be important. There is an indirect MA• control route, however, as MA• yields Br^- via reaction 15. The concentrations of H^+ and BrO_3^- are held constant in the simulations to decrease computation time, and these species, *as well as* Br^-, are not present in the CSTR feedstream, which contains only MA and Ce(III). Some previous simulations[18,21,22] had relatively high amounts of Br^- being pumped into the reactor, even though Br^- was not explicitly added to the Texas feedstream. The constant values of $[BrO_3^-]$ and $[H^+]$ in the CSTR were the mixed feedstream concentrations of the Texas experiments since these are so high that only small fractions of the BrO_3^- and H^+ are consumed even at low flow rates.

The source of the rate constants used is indicated in Table I. All are experimental values except k_{13}, k_{14}, and k_{15}, which were adjusted within reasonable limits to reproduce the experimental behavior. Reactions 13, 14, and 15 each represent a class of

(22) Lindberg, D.; Turner, J. S.; Barkley, D. *J. Chem. Phys.* **1990**, *92*, 3238.
(23) Field, R. J.; Körös, E.; Noyes, R. M. *J. Am. Chem. Soc.* **1972**, *94*, 8649.
(24) Györgyi, L.; Turányi, T.; Field, R. J. *J. Phys. Chem.* **1990**, *94*, 7162.
(25) Ruoff, P.; Varga, M.; Körös, E. *Acc. Chem. Res.* **1988**, *21*, 326.
(26) Field, R. J.; Noyes, R. M. *J. Chem. Phys.* **1974**, *60*, 1877.
(27) (a) Tomita, K. In *Chaos*; Holden, A. V., Ed.; Princeton University Press: Princeton, NJ 1986, and references therein. (b) Schreiber, I.; Marek, M. *Physica D* **1982**, *5D*, 258; *Phys. Lett.* **1982**, *91*, 263.
(28) Crowley, M. F.; Field, R. J. *J. Phys. Chem.* **1986**, *90*, 1907; *Lect. Notes Biomath.* **1986**, *66*, 68.
(29) Villermaux, J. *Annu. Rev. Chem. Eng.*, submitted, and references therein.
(30) Györgyi, L.; Field, R. J. *J. Chem. Phys.* **1989**, *91*, 6131.
(31) Györgyi, L.; Field, R. J. *J. Chem. Phys.* **1990**, *93*, 2159.
(32) Field, R. J.; Försterling, H.-D. *J. Phys. Chem.* **1986**, *90*, 5400.
(33) Försterling, H.-D.; Murányi, Sz.; Noszticzius, Z. *J. Phys. Chem.* **1990**, *94*, 2915.
(34) Försterling, H.-D.; Murányi, Sz.; Noszticzius, Z. In *Proceedings of the International Conference on Dynamics of Exotic Phenomena in Chemistry*, Hajduszoboszló, Hungary. *React. Kinet. Catal. Lett.* **1990**, *42*, 217.

TABLE I: Chaotic Model of the Belousov-Zhabotinsky Reaction[a,b]

reaction	rate constant	ref
Inorganic Subset		
1. $HOBr + Br^- + \{H^+\} \rightarrow Br_2 + \{H_2O\}$	6.0E+8 M^{-1} s^{-1} [c]	45
2. $Br_2 + \{H_2O\} \rightarrow HOBr + Br^- + \{H^+\}$	2.0 s^{-1}	45
3. $Br^- + HBrO_2 + \{H^+\} \rightarrow 2HOBr$	5.2E+5 M^{-1} s^{-1}	32,24
4. $Br^- + \{BrO_3^-\} + \{2H^+\} \rightarrow HOBr + HBrO_2$	0.01352 s^{-1}	32, 24
5. $HOBr + HBrO_2 \rightarrow Br^- + \{BrO_3^-\} + \{2H^+\}$	3.2 M^{-1} s^{-1}	32
6. $2HBrO_2 \rightarrow \{BrO_3^-\} + HOBr + \{H^+\}$	3.0E+3 M^{-1} s^{-1}	32
7. $\{BrO_3^-\} + HBrO_2 + \{H^+\} \rightarrow 2BrO_2^\bullet + \{H_2O\}$	0.858 s^{-1}	32, 24
8. $2BrO_2^\bullet + \{H_2O\} \rightarrow \{BrO_3^-\} + HBrO_2 + \{H^+\}$	4.2E+7 M^{-1} s^{-1}	32
9. $Ce^{3+} + BrO_2^\bullet + \{H^+\} \rightarrow HBrO_2 + Ce^{4+}$	1.612E+4 M^{-1} s^{-1}	32, 24
10. $HBrO_2 + Ce^{4+} \rightarrow Ce^{3+} + BrO_2^\bullet + \{H^+\}$	7.0E+3 M^{-1} s^{-1}	32, 24
Reactions Involving Organic Species		
11. $MA + Br_2 \rightarrow BrMA + Br^- + \{H^+\}$	40.0 M^{-1} s^{-1}	46
12. $MA + HOBr \rightarrow BrMA + \{H_2O\}$	8.2 M^{-1} s^{-1}	47
13. $MA + Ce^{4+} \rightarrow MA^\bullet + Ce^{3+} + \{H^+\}$	0.3 M^{-1} s^{-1}	35[d]
14. $BrMA + Ce^{4+} \rightarrow Ce^{3+} + Br^- + \{products\}$	30.0 M^{-1} s^{-1}	36[d]
15. $MA^\bullet + BrMA \rightarrow MA + Br^- + \{products\}$	2.4E+4 M^{-1} s^{-1}	24[d]
16. $MA^\bullet + Br_2 \rightarrow BrMA + Br^\bullet$	1.5E+8 M^{-1} s^{-1}	48, 24
17. $MA^\bullet + HOBr \rightarrow Br^\bullet + \{products\}$	1.0E+7 M^{-1} s^{-1}	48, 24
18. $2MA^\bullet \rightarrow MA + \{products\}$	3.0E+9 M^{-1} s^{-1}	49[e]
19. $Br^\bullet + MA \rightarrow Br^- + MA^\bullet + \{products\}$	1.0E+5 M^{-1} s^{-1}	24

[a] $[H_2O]$ = 55 M, $[BrO_3^-]$ = 0.1 M, and $[H^+]$ = 0.26 M are included in the appropriate rate constants. The literature values of the rate constants (if they exist) can be obtained by dividing the value presented here by the constant concentrations. Mixed feed concentrations: $[MA]_0$ = 0.25 M, $[Ce^{3+}]_0$ = 0.000 833 M. Together with the constant concentrations of $[BrO_3^-]$ and $[H^+]$, these are exactly the experimental conditions from refs 12 and 13. [b] Values of the variables on a chaotic attractor at k_f = 3.06E-4: $[Br^-]$ = 1.42745E-06, $[HBrO_2]$ = 2.85055E-07, [HOBr] = 6.13549E-10, $[Br_2]$ = 4.20280E-08, $[Ce^{3+}]$ = 8.30152E-04, $[Ce^{4+}]$ = 2.84792E-06, $[BrO_2^\bullet]$ = 3.09064E-08, [BrMA] = 1.20977E-03, [MA] = 2.47010E-01, $[MA^\bullet]$ = 3.98455E-09, $[Br^\bullet]$ = 1.01791E-12. [c] Read as 6.0×10^8 M^{-1} s^{-1}. [d] Adjusted in this work. [e] Rounded in this work.

reactions. Reaction 13 represents reductions of Ce(IV) without direct production of the inhibitor species Br^-. The literature value[35] of k_{13} with MA is 0.23 M^{-1} s^{-1} and is expected to be larger for other intermediates, e.g., $HOCH(COOH)_2$ and $O{=}C(COOH)_2$. Reaction 14 allows part of the products of reaction 13 to continue on to produce Br^-. This type of reaction is discussed in detail elsewhere,[24] and the rate constant used here is reasonable on the basis of that discussion. The processes by which Br^- is directly produced by Ce(IV) from BrMA are represented by reaction 15. The value of k_{15} used here is about 300 times larger than the experimental value[36] for the oxidation of BrMA by Ce(IV). This discrepancy is not surprising since reactions of derivatives of MA or BrMA with Ce(IV), some presumably leading to Br^-, are omitted from the mechanism. Furthermore, it may be[24] that freshly oxidized Ce(IV) reacts with BrMA faster than Ce(IV) that is equilibrated with the H_2SO_4 medium. We also point out that $BrMA^\bullet$ may be[24,37] a strongly inhibiting species and that this effect could be mimicked by the high value of k_{15}. We made no effort to search for other sets of k_{13}–k_{15} containing a lower value of k_{15} that might work equally well.

The introduction of BrMA and its reactions makes this model an extended SNB[20] model with the correct roles assigned to HOBr and Br_2 and with the values of *both* k_5 and f parametrized through [BrMA].

Results

The model shows a wealth of complex behaviors which contain as a subset virtually all experimentally observed phenomena at low flow rates. Figure 1 shows the comparison of the variety of behaviors seen experimentally[13] with the corresponding simulation results. The experimental behavior at the lowest flow rate shown is a simple periodicity consisting of one small-amplitude and one large-amplitude oscillation. This is called 1^1 periodicity where the base refers to the number of large peaks and the superscript refers to the number of small peaks per cycle. This notation is the same as used to describe[13] some of the experimental results. (There is another notation for the periodic–chaotic sequences

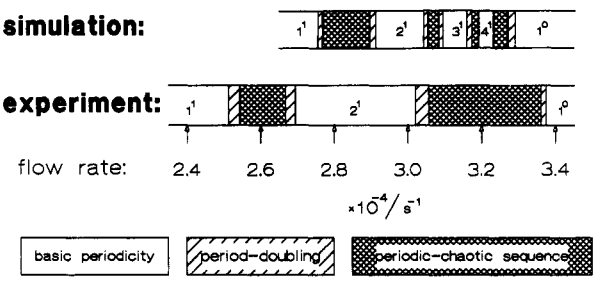

Figure 1. Comparison of phenomena found in simulations and in experiments in the flow rate region where experimental data are available. The schematic representation of the experimental results is based on Figure 2 of ref 13.

discussed here in which 1^0 is referred to as P_1, 1^1 as P_2, 1^2 as P_3, the region between 1^0 and 1^1 is called C_1, the region between 1^1 and 1^2 is called C_2, etc.) A period-doubling cascade of the 1^1 periodicity occurs as the flow rate is increased and is followed by a window containing both complex periodicities and chaos. A reversed cascade of period-doubling bifurcations occurs at even higher flow rates resulting in 2^1 periodicity. This limit cycle loses stability, again via period doubling, and another periodic–chaotic window is approached as the flow rate continues to increase. Another reversed cascade of period-doubling bifurcations occurs on the high-flow-rate side of this window, and a region is approached where only regular, periodic oscillations with uniformly large peaks are observed (1^0 limit cycle).

Stable long-term behaviors found in simulations are displayed in Figures 1 and 2. Figure 1 shows only the relatively high-flow-rate region where a comparison with experimental results is possible. Figure 2 shows all results obtained so far with this model. The symbolism introduced in ref 30 is used. The simulated sequence of periodic windows and the waveforms of periodic and chaotic oscillations in Figure 1 are very similar to those seen in the Texas experiments at the same flow rates. Indeed, the reproducibility of these experiments is such that there are smaller differences between the Texas experiments and these simulations than there are between the Texas and Münster–Schneider[15] experiments.

The first period-doubling bifurcation of the 1^0 limit cycle as the flow rate is decreased from its highest value in the simulations occurs almost where it does in the experiments. A sequence of

(35) Försterling, H.-D.; Idstein, H.; Pachl, R.; Schreiber, H. *Z. Naturforsch.* **1984**, *39A*, 993.
(36) Försterling, H.-D.; Pachl, R.; Schreiber, H. *Z. Naturforsch.* **1987**, *42A*, 963.
(37) Stuk, L.; Roberts, J.; McCormick, W. D.; Noszticzius, Z. *J. Phys. Chem.* **1990**, *94*, 6734.

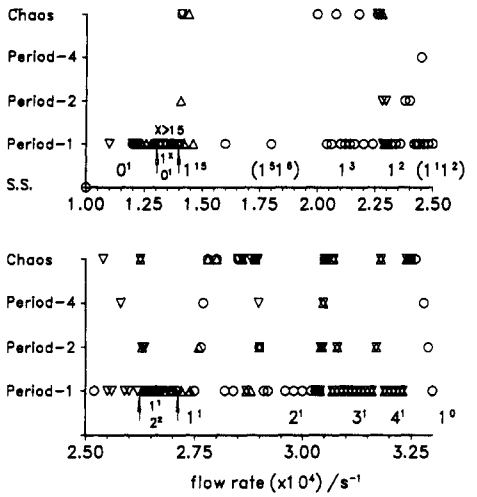

Figure 2. Schematic representation of the results of numerical simulations with the model in Table I. On the ordinate SS means steady state and period-1 means a basic periodicity, while period-2 and period-4 denote limit cycles evolved from a basic periodicity via period-doubling bifurcations. Some of the major basic periodicities are indicated and are characterized by the notation L^S where L is the number of large peaks and S is the number of smaller peaks within a period. The distinction between large and small peaks is unambiguous in most cases. Circles indicate simulation results obtained by using arbitrary initial conditions and regular triangles show results of a series of runs with gradually increasing flow rate, while inverted triangles indicate consecutive simulations with decreasing flow rate. Some of the bistable regions are enclosed by arrows, and the types of the coexisting attractors are indicated.

periodic and chaotic states then is observed. The flow rate grid of the simulations is fairly coarse, but several simple periodicities can be identified within the periodic–chaotic windows. These include a 4^1 and then a rather wide 3^1 periodicity. A period-doubling bifurcation is observed on both sides of the 3^1 limit cycle. A 2^1 periodicity is found when the flow rate is further decreased, as in experiments. There are several strange attractors between the 1^0 and 2^1 limit cycles characterized by next-maximum maps very similar to those observed experimentally. Most of these maps are one-humped and single-valued except in small regions at the tail of the hump where the next-maximum value cannot be unambiguously determined on the basis of the previous one. Similar maps were encountered[38,39] experimentally. These regions of ambiguity often are so narrow that experimental noise would make it impossible to detect them. The log [Br^-] time series of one of these strange attractors is displayed in Figure 3A along with the next-maximum map derived from it in Figure 3B and its three-dimensional image in Figure 3C. A fairly wide area of periodic–chaotic windows follows as the flow rate is decreased out of the 2^1 region before the observed 1^1 periodicity is approached through a reversed cascade of period-doubling bifurcations. A typical next-maximum map from these latter aperiodic regions is shown in Figure 4A at $k_f = 2.890 \times 10^{-4}$ s^{-1}. Contrary to its single-valued appearance, this map is, in fact, double-valued at high log ($[Br^-]_{max}$).

Figure 2 displays simulation results at lower flow rates than shown in Figure 1. There is a sequence of period-doubling bifurcations at the low-flow-rate end of the 1^1 periodicity, and a region appears with more complex limit cycles and occasional chaos. When the flow rate is reversed after the accumulation point of the period-doubling cascade, reversed period-doubling bifurcations lead to a 2^2 periodicity, which coexists with the 1^1 limit cycle over a small flow rate range, as is shown in Figure 2. More narrow bistable regions appear as the flow rate is further decreased. Several of these hysteresis phenomena involve two limit cycles, one containing twice as many peaks as the other but with the same

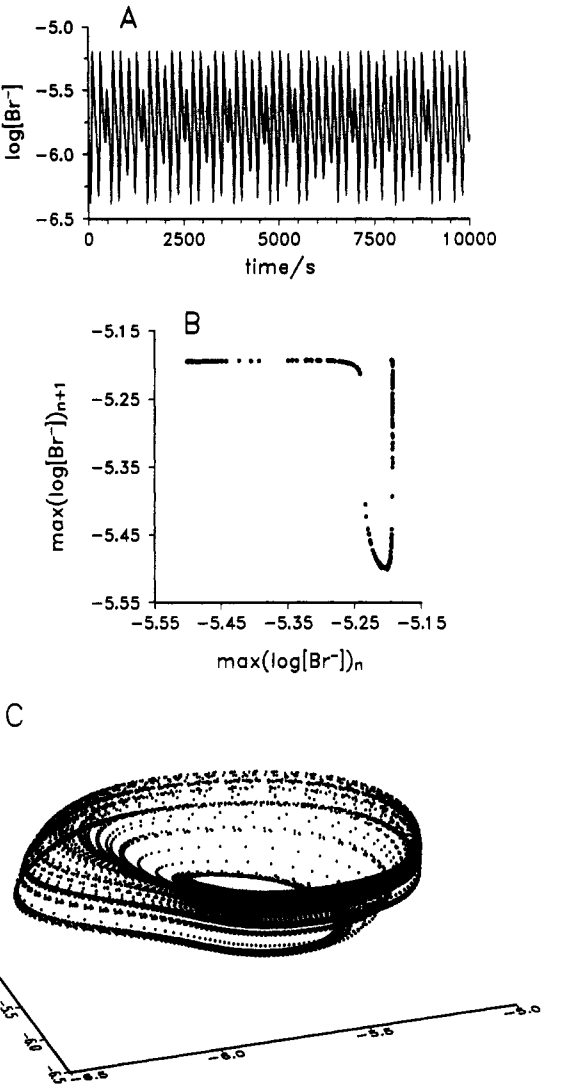

Figure 3. Chaotic behavior obtained at $k_f = 0.000\,3071$ s^{-1}: (A) simulated time series of log [Br^-]; (B) next-maximum map constructed from the time series of log [Br^-]; (C) three-dimensional image of the same strange attractor. The vertical axis is log [BrMA] and the "longer" horizontal axis is log [Br^-] while the "shorter" one is log [Ce(IV)]. Consecutive symbols (dots) are separated by 2 s.

large/small ratio. An increasing number of small peaks per cycle characterize the region below the 1^1 periodicity. There seems to be less chaos and more periodicity at lower flow rates than in the periodic–chaotic windows discussed above, and Figure 4B,C shows that the chaotic next-maximum maps become increasingly complex. The Poincaré sections in Figure 5A,B indicate chaotic motion on the remains of a broken torus.

A sharp transition to small-amplitude sinusoidal oscillations (0^1) also seen experimentally[38,39] occurs at even lower flow rates between $k_f = 1.34 \times 10^{-4}$ s^{-1} and $k_f = 1.32 \times 10^{-4}$ s^{-1}. Increasing the flow rate at this point reveals (Figure 2) a hysteresis between small-amplitude sinusoidal oscillations and the mixed-mode oscillations seen before. The sinusoidal oscillations lose stability at $k_f \approx 1.405 \times 10^{-4}$ s^{-1} and abruptly fall into the mixed-mode behavior. Very long, apparently quasiperiodic transients in this region, however, reveal the presence of a weakly repelling torus which identifies this transition as a subcritical secondary Hopf bifurcation. At the lower flow rate end of the 0^1 region, the small oscillations disappear via a Hopf bifurcation between $k_f = 1.1 \times 10^{-4}$ s^{-1} and $k_f = 1.0 \times 10^{-4}$ s^{-1}, and a reduced steady state is observed as in the experiments.

Discussion

Experiments must finally decide whether the Texas chaos results primarily from the presence of inhomogeneities in the CSTR or

(38) McCormick, W. D. Personal communication.
(39) Coffman, K. G. Ph.D. Thesis, University of Texas at Austin, Austin, TX, 1986.

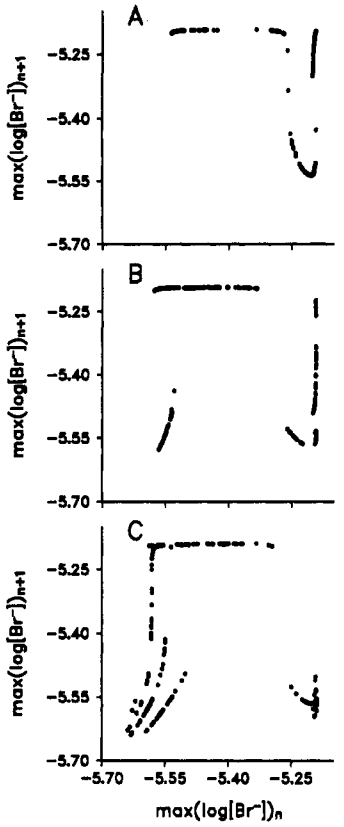

Figure 4. Series of next-maximum maps constructed from chaotic log [Br^-] time series obtained as the flow rate is decreased: (A) k_f = 0.000 289 s^{-1}, (B) k_f = 0.000 254 s^{-1}, (C) k_f = 0.000 208 s^{-1}.

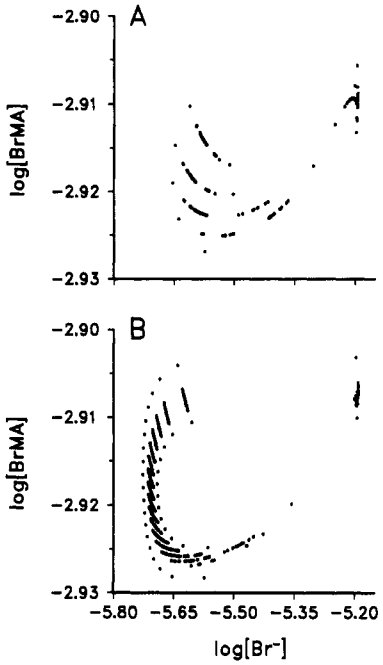

Figure 5. Two Poincaré sections indicating the presence of the fractal remains of a torus as the source of aperiodicity. The Poincaré plane is defined by log [Ce(IV)] = −5.7, and only the crossings with d[Ce(IV)]/dt < 0 are indicated. (A) k_f = 0.000 208 s^{-1}; (B) k_f = 0.000 141 s^{-1}.

from the combination of the homogeneous chemical kinetics with the CSTR flow. These simulations and the findings of Münster and Schneider,[15] however, suggest that it is the latter which results in aperiodicity in the low-flow-rate experiments considered here. Since experimental attempts to reproduce[15] the chaos found at much higher flow rates have failed, and because some aperiodic experiments show stirring rate dependence,[10] external coupling,

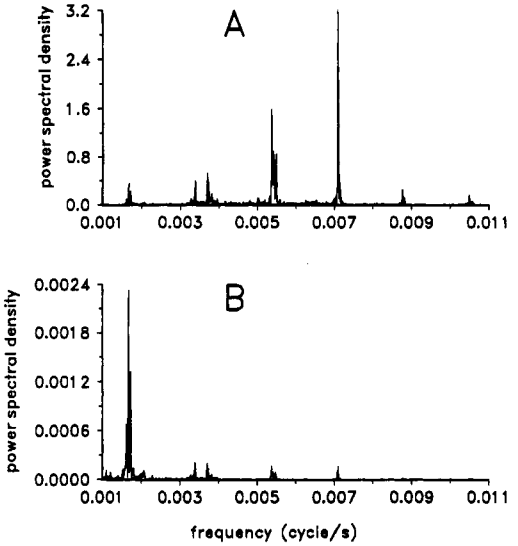

Figure 6. Power spectra (estimated with the periodogram method) prepared from the log [Br^-] (A) and from the log [BrMA] (B) time series at k_f = 0.000 208 s^{-1} (chaotic state). Note the difference in the fundamental frequencies.

that is, the presence of inhomogeneities in the reactor, still seems to be a viable explanation for certain other chaotic BZ-CSTR experiments.

Our analysis is based on [BrMA] as a bifurcation parameter for the Oregonator core and its cycling with a frequency different from that of the Oregonator core because of its involvement in a second negative feedback loop. Tests were carried out to demonstrate the effect of [BrMA] as a bifurcation parameter. If 0.001 M BrMA is introduced into the feedstream at k_f = 0.000 33 s^{-1} (high-flow-rate end of the region studied here, 1^0 oscillations), the system immediately goes into its reduced steady state. Less added BrMA causes complex oscillations and chaos, as in experiments.[13b]

The second negative feedback loop emerges at low flow rates when [BrMA] is close to the critical value above which the reduced state of the Oregonator core is stable. As soon as its concentration overshoots this critical value, the Oregonator core is attracted to its reduced steady state where BrMA production stops. This allows the flow to decrease [BrMA] below the critical value where the Oregonator core resumes oscillation, and BrMA is again produced rapidly during the oxidized excursions. The two power spectra in Figure 6A,B obtained at k_f = 0.000 208 s^{-1} (chaotic behavior) show that [Br^-] and [BrMA] oscillate with different fundamental frequencies. In general, the Oregonator core variables oscillate with a different fundamental frequency than [BrMA]. The frequency of [BrMA] oscillations introduced by this second feedback loop may not always entrain with the frequency of the Oregonator core. This separation of frequencies results because the time needed to return [BrMA] below the critical value depends essentially completely on the flow rate and the value of $[BrMA]_{max}$ rather than on the concentrations of the components of the Oregonator core. The role of the CSTR flow in the removal of BrMA is verified by a series of simulations at k_f = 0.000 33 s^{-1} where the observed behavior is 1^0 oscillations. The rate at which BrMA alone is washed out of the system, i.e., k_f exclusively for BrMA, was then decreased. The result was a sequence of dynamic behaviors strikingly similar to that observed when k_f was changed, affecting both the inflow and the outflow of *all* components. These results show that the major effect of changing the flow rate is, in fact, adjusting the first-order decay of BrMA.

These qualitative guidelines allow us to interpret the major sequence of periodic and chaotic states in the low-flow-rate region of complexity studied here. At the high-flow-rate end of this region, the fast outflow of BrMA requires several large-amplitude oscillations to "pump" [BrMA] above its critical value, and the time spent in the neighborhood of the reduced state is short. Both periodic and chaotic states in this region are dominated by

large-amplitude peaks. As the flow rate is decreased, one oxidative excursion produces enough BrMA to temporarily stabilize the reduced state of the Oregonator core, and with decreasing flow rate more and more time is spent spiraling around this fixed point.

Noszticzius et al.[13b] have found that adding $HBrO_2$ or its precursor HCHO to the feedstream decreases the amount of complexity in this region (chaos may disappear), while addition of BrMA or its precursor, HOBr, expands the flow rate region of complexity. These phenomena also are understood easily in terms of the above discussion. Addition of $HBrO_2$ promotes the oxidized state of the system, thus increasing the critical [BrMA] value required for the reduced state to become attracting. This effectively shifts the complexity to lower flow rates or possibly eliminates it. On the other hand, if BrMA is pumped into the CSTR the first-order rate of removal of BrMA by the flow decreases from $-k_f$[BrMA] to $k_f([BrMA]_0-[BrMA])$, effectively shifting the high-flow-rate border of mixed-mode oscillations and chaos to even higher flow rates. Qualitatively similar but larger than the experimental effects were obtained in our simulations when BrMA was added to the feedstream.

Of course, the complex nature of the coupling between the Oregonator core frequency and the frequency of the cycling BrMA does not allow this qualitative reasoning either to provide detailed information on the dynamics or to prove the existence of chaos. These questions must be decided in a model this size by numerical experimentation. Simplification of this model is under way to better understand its dynamics. The reasoning and the qualitative guidelines outlined above, however, are useful in understanding the chemistry of such a complex system and in designing chemical mechanisms for similar systems.

We note that a negative feedback loop emerges in an analogous manner at high flow rates when BrMA is washed out, forcing the Oregonator core of the system into the oxidized state where BrMA is continuously produced. This pushes [BrMA] back to values where the Oregonator core is oscillatory, and the rate of BrMA production is less. This gives rise to the complexity observed in experiments at high flow rates. A major difference between the low- and high-flow-rate complexity is that the time spent in the neighborhood of the oxidized steady state does depend on the values of the Oregonator core variables as they determine the rate of BrMA production. We expect this to cause the two frequencies to readily entrain, thus making complex periodicity more likely than chaos.

Numerical Aspects

A VAX 8600 or a 25-MHz "386" PC with a Weitek 3167 coprocessor were used for all numerical integrations, which were carried out using the program SIMULATE developed by one of us[40] based on the numerical integrator ROW4S.[41,42] Usually a relative error tolerance between 10^{-5} and 10^{-4} was used; spot checks with 10^{-6} gave identical, stable long-term behavior. There was, however, some dependence of the length of the transients on the error tolerance. An error tolerance of 10^{-7} resulted in unacceptable computing times on the VAX 8600; e.g., over 2 days computing time was required to integrate the model to 150 000 s. The error control in ROW4S is different from that in more commonly used integrators like LSODE[43] or GEAR.[44] While 10^{-7} may seem to be rather large tolerance in these latter cases, for ROW4S it represents a practical lower limit. Independent simulations using LSODE reproduced several of the periodic and chaotic behaviors reported here. The differential equations were integrated for at least 70 000 s and up to 150 000 s at the lowest flow rates used before data collection in order to avoid transients. The end point of the preceding calculation was used to start the next simulation when searching for hysteresis effects by gradually changing the flow rate. This mimics the experimental situation.

The phenomena seen in the simulations were classified on the basis of visual examination of the time series, the log [BrMA] vs log [Br^-] phase portrait, the next-maximum map constructed from the log [Br^-] time series, and the Poincaré sections constructed as described in the legend for Figure 5. These methods, especially the last two, are very efficient for identifying transients and complex periodic behavior. Although we recognize the importance of other methods, e.g., calculating the correlation dimension or the spectrum of Lyapunov characteristic exponents of experimental data, in the case of noise-free, simulated data, the above-mentioned graphical procedures are fast and reliable.

We encountered two major difficulties in identification of the stable long-term behavior. One of them was the appearance of extremely long (sometimes more than 100 000 s) transients, which may appear even when the initial concentrations are chosen from an attractor at a neighboring flow rate. Long transients are often found close to bifurcation points, especially when the stable long-term behavior is a weakly attracting, complex periodicity. This indicates that great care should be taken when judging an experimental attractor to be periodic or chaotic since it is impractical experimentally to allow more than 10 000–20 000 s for transients to decay. Bistable regions generated the other difficulty. Spontaneous branch switching occurred in many cases even when the flow rate was changed by less then 1%. This indicates that the position of the separatrix between the two attractors must depend strongly on the flow rate so that parts of one attractor may fall into the region of attraction of the other at a nearby flow rate value.

Conclusion

Simulations cannot prove the validity of the model they are based on, but they can be very useful in testing theoretical ideas. Our results suggest that the low-flow-rate complexity and chaos in the Texas experiments can be explained as the result of the homogeneous chemical kinetics and that its source in the chemical mechanism is the coupling between two frequency sources: one being the Oregonator core of the mechanism and the other originating in the negative feedback loop emerging when the concentration of bromomalonic acid approaches a value above which the reduced steady state of the Oregonator core is stable.

The model of the BZ reaction introduced in this paper reproduces the periodic–chaotic sequences found at low flow rates in the Texas BZ-CSTR experiments. In particular, the sequence of major periodic and chaotic states, the period-doubling bifurcations leading from periodicity to chaos, the regular, 1^0-type oscillations at the highest flow rates, the character of the major limit cycles with increasing number of small peaks per period as the flow rate is decreased, the discontinuous switch to small-amplitude, sinusoidal 0^1-type oscillations at low flow rates, the reduced steady state at the lowest flow rate used, the waveform and structure associated with the strange attractors, the flow rate range, and reactant concentrations where these phenomena occur are all satisfactorily simulated. If one considers the relatively poor independent reproducibility of these experiments, then a better fit than this cannot be hoped for.

There are some subtle differences between the Texas experiments and these simulations. The flow rate range between the 1^1 and 1^0 periodicity in the simulations is only about 60% of the experimental. It is difficult to discern from the published experimental work[12,13] how typical the well-known single-valued,

(40) Györgyi, L. Department of Chemistry, Department of Chemistry, University of Montana, Missoula, MT 59812. On leave from: Institute of Inorganic and Analytical Chemistry, Eötvös Lóránd University, Budapest-112, P.O. Box 32, H-1518, Hungary.
(41) Gottwald, B. A.; Wanner, G. *Computing* **1981**, *26*, 355.
(42) Valkó, P.; Vajda, S. *Comput. Chem.* **1985**, *8*, 255.
(43) Hindmarsh, A. C. Livermore Solver for Ordinary Differential Equations. Technical Report No. UCID-3001; Lawrence Livermore Laboratory: Livermore, CA, 1972.
(44) Gear, C. W. *Numerical Initial Value Problems in Ordinary Differential Equations*; Prentice-Hall: Englewood Cliffs, NJ, 1972; Chapter 11.
(45) Kshirsagar, G.; Field, R. J. *J. Phys. Chem.* **1988**, *92*, 7074.
(46) Försterling, H.-D.; Field, R. J.; Györgyi, L. Unpublished result at 25 °C.
(47) Pachl, R. Ph.D. Thesis, Philipps-Universität Marburg, FRG, 1989.
(48) Försterling, H.-D.; Noszticzius, Z. *J. Phys. Chem.* **1989**, *93*, 2740.
(49) Brusa, M. A.; Perissinotti, L. J.; Colussi, A. J. *J. Phys. Chem.* **1985**, *89*, 1572.

one-humped, next-maximum map is in this region. More complex maps certainly do occur in the experiments.[38,39] We never saw a truly single-valued simulated next-maximum map; nevertheless, the maps in Figures 3b and 4a would certainly appear single-valued in the presence of even a low level of experimental noise, and there are indications[39] that all experimental maps may consist of multiple sheets. We did not make a systematic attempt to search for a single-valued map by carefully tuning the flow rate or the adjustable rate constants. The simulations seem to contain larger domains of periodicity than do the experiments, although it is not clear from published experimental results how much periodicity is contained in the periodic–chaotic windows. The experimental work of Coffman et al.[12,39] certainly suggests the presence of a large variety of complex limit cycles in the regions between the major periodicities. Several bistable regions between two different periodicities or a periodicity and a strange attractor were found in the simulations at flow rates lower than shown in Figure 1. We cannot be certain from the experimental results available to us whether these hystereses occur in the real system. The same is true of the transition between sinusoidal and mixed-mode oscillations, which we found in the simulations to be a subcritical, secondary Hopf bifurcation. It was not possible to identify the nature of this transition in experiments,[39] nor could it be proved whether hysteresis exists due to difficulties associated with the large residence time where the transition occurs.

Note added in proof: Noszticzius[50] verified that the same bistability exists experimentally.

Even if these phenomena prove inconsistent with the experiments, the convincing agreement in the major characteristics of the dynamics suggests that the discrepancies may well be removed simply by choosing other values for k_{13}–k_{15}. The numerical difficulties mentioned above, however, indicate that in some cases the experimental phenomena may be transient or artifacts of the coupling of mixing and noise with the extremely sensitive BZ dynamics. Thus, it is unclear how close one can expect experiments to match simulations where the stable long-term behavior can almost always be elucidated.

Acknowledgment. This work was supported by the National Science Foundation under Grant CHE-8822886. We thank F. W. Schneider and Th.-M. Kruel of the University of Würzburg, FRG, William D. McCormick of the University of Texas, Austin, and Andrzej Kawczynski of the Institute of Physical Chemistry of the Polish Academy of Sciences for valuable discussions and the University of Montana Computing and Information Services for computing time and technical support. We also thank reviewer 1 for many useful comments and suggestions.

(50) Noszticzius, Z. Unpublished results. We thank Professor Noszticzius for communicating his results to us.

Competition between Silver Ions and Oxybromine Species for Bromide Ions in the Silver-Perturbed Belousov–Zhabotinskii Reaction

Jay Roberts, Linda Stuk, and William D. McCormick*

Center for Nonlinear Dynamics and Department of Physics, University of Texas at Austin, Austin, Texas 78712 *(Received: July 11, 1990; In Final Form: October 26, 1990)*

We investigated the relative rates of bromide consumption by silver ions and by the oxybromine species of the Belousov–Zhabotinskii reaction. Our results indicate that the consumption of bromide by silver is too slow to suppress bromide control of the oscillating reaction.

Introduction

The Belousov–Zhabotinskii reaction is the most thoroughly investigated oscillating chemical reaction. It has become one of the most important examples of a nonlinear dynamical system for which detailed studies are feasible.[1,2] Much attention has therefore been focused on the details of its chemistry, and in particular the control mechanisms that inhibit the autocatalytic step,[3-7] making complex behavior possible.

The major control species is bromide, as demonstrated in the landmark paper of Field, Körös, and Noyes.[8] To study the possibility of other control mechanisms, several investigators have added silver ions to precipitate the bromide. A review of these experiments is given in ref 9. There has been a controversy, also explained in ref 9, about whether the rate of silver bromide precipitation is fast enough for this method to be effective. Bromide production is a dynamic process, so the rate of precipitation is more important than the equilibrium solubility constant. It has been pointed out[10] that the maximum concentration of silver ions that can be used without precipitating silver bromate is fairly low, since the solubility product[11] for $AgBrO_3$ is 5.8×10^{-5}. Hence the rate of precipitation cannot be made arbitrarily high.

The effect of silver perturbations on the BZ reaction depends on the relative rates of the following reactions:

$$Br^- + BrO_3^- + 2H^+ \rightleftharpoons HBrO_2 + HOBr \quad (1)$$

$$Br^- + HBrO_2 + H^+ \rightleftharpoons 2HOBr \quad (2)$$

$$Br^- + HOBr + H^+ \rightleftharpoons Br_2 + H_2O \quad (3)$$

$$Br^- + Ag^+ \rightleftharpoons AgBr(s) \quad (4)$$

Equation 4 is not elementary, as the precipitation requires several steps to form molecules, complexes, and nuclei.[12-14]

* To whom correspondence should be addressed.

(1) Field, R. J.; Burger, M. *Oscillations and Traveling Waves in Chemical Systems*; Wiley: New York, 1985.
(2) Swinney, H. L.; Roux, J. C. In *Nonequilibrium Dynamics in Chemical Systems*; Vidal, C., Pacault, A., Eds.; Springer: Berlin, 1984.
(3) Györgyi, L.; Turányi, T.; Field, R. J. *J. Phys. Chem.* **1990**, *94*, 7162.
(4) Försterling, H. D.; Noszticzius, Z. *J. Phys. Chem.* **1989**, *93*, 2740.
(5) Murányi, S.; Försterling, H. D. *Z. Naturforsch.* **1990**, *45a*, 135.
(6) Försterling, H. D.; Murányi, S.; Noszticzius, Z. *J. Phys. Chem.* **1990**, *94*, 2915.
(7) Stuk, L.; Roberts, J.; McCormick, W. D.; Noszticzius, Z. *J. Phys. Chem.* **1990**, *94*, 6734.
(8) Field, R. J.; Körös, E.; Noyes, R. M. *J. Am. Chem. Soc.* **1972**, *94*, 8649.
(9) Noyes, R. M.; Field, R. J.; Försterling, H. D.; Körös, E.; Ruoff, P. *J. Phys. Chem.* **1989**, *93*, 270.
(10) Noszticzius, Z.; McCormick, W. D. *J. Phys. Chem.* **1987**, *91*, 4430.
(11) *CRC Handbook of Chemistry and Physics*, 50th ed.; Chemical Rubber Company: Cleveland, 1969.

0022-3654/91/2095-3165$02.50/0